JOURNAL OF Materials CHEMISTRY

Adsorption and sensing properties of microporous layered tin sulfide materials

Tong Jiang,[a] Geoffrey A. Ozin,*[a] Atul Verma and Robert L. Bedard[b]

[a] *Materials Chemistry Research Group, Department of Chemistry, University of Toronto, Toronto, Ontario, Canada, M5S 3H6*

[b] *Universal Oil Product, 25 E. Algonquin Rd., Des Plaines, Illinois, 60017, USA*

The adsorption and sensing behavior of three structurally well defined microporous layered tin sulfides $R_2Sn_3S_7$, denoted DABCOH-SnS-1, ATEA-SnS-1 and TEA-SnS-1, have been explored. In the case of small non-polar guests a micropore-filling process is observed, whereas for certain larger guests an integration of micropore-filling and intercalation is found to occur. The former is controlled by the size while the latter depends on the adsorption properties of the guest molecules. It seems that guests with a propensity for hydrogen bonding are favored for intercalation. Electrical and optical responses with respect to adsorption of specific guests, such as NH_3, H_2S and alcohols, show high sensitivity, reversibility and fast reaction times that are comparable to some commercial semiconductor sensors. This makes microporous layered tin sulfides potentially interesting in environmental, industrial and biomedical monitoring.

In contrast to dense packed structures or amorphous porous materials with a broad pore size distribution, microporous materials with crystallographically defined pore systems are able to discriminate molecules based on their size and shape. This unique structural feature has made microporous materials particularly useful in applications where molecule size/shape selectivity is required, for example, in catalysis and separation science.[1] In the past decade, the design of new chemical sensing devices using microporous materials as the transducer has received growing interest.[2] It is envisaged that arrays of microporous materials with a range of pore sizes and shapes should enable the detection of target molecules, without significant interference from other molecular species. Zeolite-modified surface acoustic wave (SAW) devices and piezoelectric quartz crystal microgravimetric (QCM) type sensors have shown promise in selective detection of organic molecules.[3] In the mass-sensitive sensors, the signal transduction involves a change of resonance frequency of the quartz crystal oscillator due to a change of mass upon adsorption. Aluminophosphate molecular sieve coated capacitance sensing devices have also been reported recently.[4] As all these metal oxide-based open-frameworks are electrical insulators, it might be advantageous to employ electrically conductive open-framework materials, where the charge-transport behavior is sensitive to the identity and concentration of target molecules. Analytes could therefore be monitored by a change of resistance. As bulk tin sulfide SnS_2 is a semiconductor, it is envisaged that the microporous layered SnS-*n* families could be interesting electrical materials for chemical sensing applications.[5]

In this paper, the guest molecule adsorption and electrical/optical sensing behaviour of three structurally well defined SnS-1 materials, DABCOH-SnS-1, ATEA-SnS-1 and TEA-SnS-1, will be used for exploratory studies. Papers that describe details of the synthetic, structural and spectroscopic properties of these materials have been published recently.[6–9] In brief, their structures are all based upon $(Sn_3S_7)^{2-}$ tin sulfide layers with regular arrays of hexagonal-shaped 24-atom pores, Fig. 1. Of particular note, the $(Sn_3S_7)^{2-}$ layers in the differently templated SnS-1 materials exhibit distinct symmetry and stacking sequences, attributed to their framework flexibility. It is important to note that the $DABCOH^+$ cations in DABCOH-SnS-1 $[(DABCOH)_2Sn_3S_7]$ reside completely within the lamellar gap of the tin sulfide sheets and leave the 24-atom pores within the layer empty, while in TEA-SnS-1 $[(Et_4N)_2Sn_3S_7]$ and ATEA-SnS-1 $[(Et_4N)_{1.5}(NH_4)_{0.5}Sn_3S_7]$, the hydrocarbon chains of Et_4N^+ are well extended into the 24-atom pores. The NH_4^+ cations in ATEA-SnS-1 lie between the tin sulfide sheets.[6–9] This implies that the free pore volume present in the as-synthesized materials decreases sequentially from DABCOH-SnS-1 to ATEA-SnS-1 and TEA-SnS-1. On the other hand, these layered SnS-1 materials are also expected to be able to undergo intercalation reactions, swelling the interlamellar gap on incorporation of guest molecules. In what follows, the adsorption and sensing properties of these materials will be studied by *in situ* FTIR and UV–VIS spectroscopy, PXRD, gas adsorption and electrical conductivity measurements.

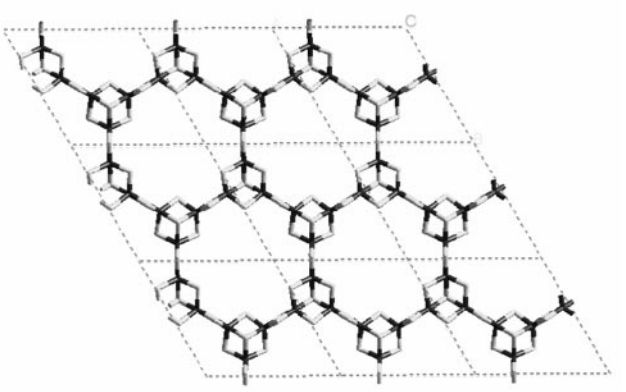

Fig. 1 A projection of the (001) plane taken from the single crystal XRD structure of the microporous layered material, ATEA-SnS-1[7]

Results

In situ FTIR measurements

The reversible adsorption–desorption of molecules in the microporous layered tin(IV) sulfides can be readily probed by *in situ* FT-mid-IR spectroscopy as demonstrated in Fig. 2 for a TEA-SnS-1 sample. The vibrational frequencies at 3564 and 3484 cm^{-1} correspond to the νOH stretching modes of the physisorbed water, denoted $(H_2O)_p$, while the sharp peak at

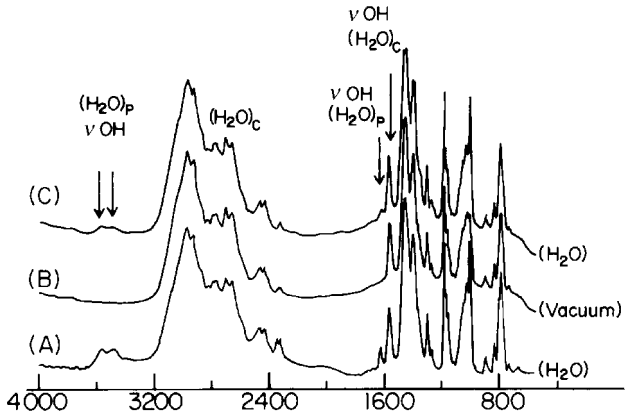

Fig. 2 FTIR spectra of TEA-SnS-1: (A) in air, (B) under vacuum, (C) re-opened to air

$1619\ cm^{-1}$ corresponds to the δHOH deformational mode. The physisorbed water molecules $(H_2O)_p$ can be easily removed by evacuating the sample at room temperature or heating the sample at 80 °C. This process is reversible over many cycles. The stretching and deformational modes for the chemisorbed water, denoted $(H_2O)_c$, appear as a broad band covering the range of about $3200–2300\ cm^{-1}$ and a sharp band at $1564\ cm^{-1}$, respectively. From a D_2O exchange study using *in situ* FTIR and TGA–MS, the chemisorbed water is found to be strongly hydrogen bonded to the framework sulfur and cannot be removed without destroying the framework of TEA-SnS-1.

The reversible adsorption of water molecules by DABCOH-SnS-1 and ATEA-SnS-1 at room temperature has also been probed by *in situ* FTIR studies. The νOH stretching bands for the physisorbed water appear at 3539 and $3431\ cm^{-1}$ in ATEA-SnS-1 and 3590 and $3420\ cm^{-1}$ in DABCOH-SnS-1, and the corresponding δHOH deformational mode at $1621\ cm^{-1}$ in the former and $1631\ cm^{-1}$ in the latter. These physisorbed water molecules can also be readily removed by evacuating the sample at room temperature. These processes are reversible and reproducible over many cycles without any measurable alterations of the properties of these materials.

When a dehydrated TEA-SnS-1 sample, devoid of physisorbed water, is exposed to H_2S and H_2Se vapors at room temperature, new vibrational modes occur at $2506\ cm^{-1}$ and $2242\ cm^{-1}$ which correspond to the physisorbed $(H_2S)_p$ and $(H_2Se)_p$, respectively, Fig. 3. The $(H_2S)_p$ and $(H_2Se)_p$ can be removed by evacuation of the sample at room temperature. Therefore, in addition to water, the TEA-SnS-1 material can also reversibly adsorb and desorb H_2S and H_2Se at room temperature. A similar experiment has been conducted using CO. Interestingly, there is no sign of adsorption of this guest molecule. The TEA-SnS-1 sample selectively adsorbs H_2O, H_2S and H_2Se but discriminates CO. In view of the smaller kinetic diameter of CO (3.76 Å)[10] compared to that of H_2Se (4 Å), the observed discrimination of CO by TEA-SnS-1 should be attributed to the adsorption behavior of CO rather than its size. Note that the kinetic diameter of the H_2Se molecule is based on the reported kinetic diameter of 3.6 Å for H_2S[10] and the relative size of Se compared with S. The former is consistently 10% larger than the latter in its atomic, covalent and ionic radii.[11]

Power X-ray diffraction

Guest-induced framework flexibility. An insight into the structural details of the R-SnS-1 materials upon adsorption has been provided by *in situ* PXRD studies. Actually, the molecular recognition ability of the SnS-*n* materials was first discovered by the observation of variable PXRD patterns of a

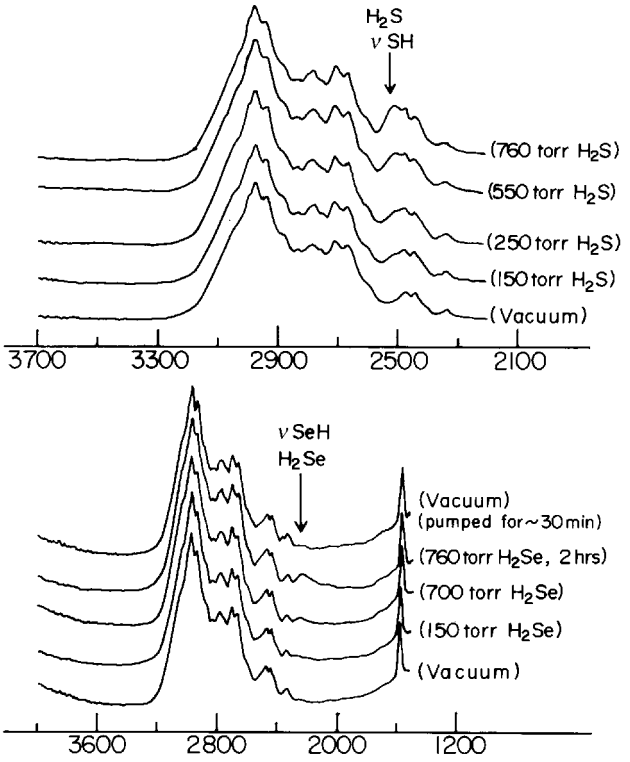

Fig. 3 *In situ* FTIR spectra of TEA-SnS-1 under vacuum and exposed to (A) H_2S and (B) H_2Se at room temperature

TEA-SnS-1 sample at different seasons of the year, as shown in Fig. 4A. Clearly, the structure of this material varies reversibly and simultaneously with the change of season. In the humid summer of Toronto, TEA-SnS-1 has a pseudo-orthorhombic unit cell in which reflections such as $h0l$ and $-h0l$ are overlapped (degenerate), *i.e.* the unit cell β angle is close to 90°. TEA-SnS-1 is crystallized in the space group $P2_1/n$, as established by single crystal (SC) XRD analysis.[7] In contrast, in the dry winter TEA-SnS-1 adopts a monoclinic unit cell, in which the $h0l$ and $-h0l$ reflections are split (non-degenerate). The reversible change of the unit cell parameters is believed to originate from the change of atmospheric humidity. An *in situ* PXRD water adsorption study, Fig. 4B, confirmed this proposal. The unit cell of TEA-SnS-1 under vacuum displays the largest monoclinic β angle (95.26°) and the smallest unit cell volume (2667 Å^3), Table 1, while a water-saturated TEA-SnS-1 sample exhibits the largest unit cell volume (2823 Å^3) and the smallest β angle (90.11°), essentially a pseudo-orthorhombic unit cell. Depending upon the humidity and amount of the physisorbed water molecules in the sample, the unit cell dimensions and β angle of TEA-SnS-1 can adopt any intermediate value between those of the monoclinic and pseudo-orthorhombic end-members. The unit cell volume is found to expand by as much as 5.8% between these two end-members which corresponds to a total volume of 156 Å^3. The decrease of the monoclinic β angle from 95.26° to 90° *i.e.* a pseudo-orthorhombic unit cell, increases the symmetry of the entire structure. This process modifies the shape of the 24-atom pores in the tin sulfide sheets, the positions of the Et_4N^+ template, and the registry of the porous tin sulfide layers with respect to each other.

Void-filling and/or intercalation? An inspection of the unit cell parameters of the two end-members of TEA-SnS-1, listed in Table 1, reveals that the expansion of the unit cell occurs mainly along the crystallographic *c* and *a* directions, the ***b*** parameter remains almost invariant. The microporous layers of TEA-SnS-1 reside on the (202) Miller plane, the expansion

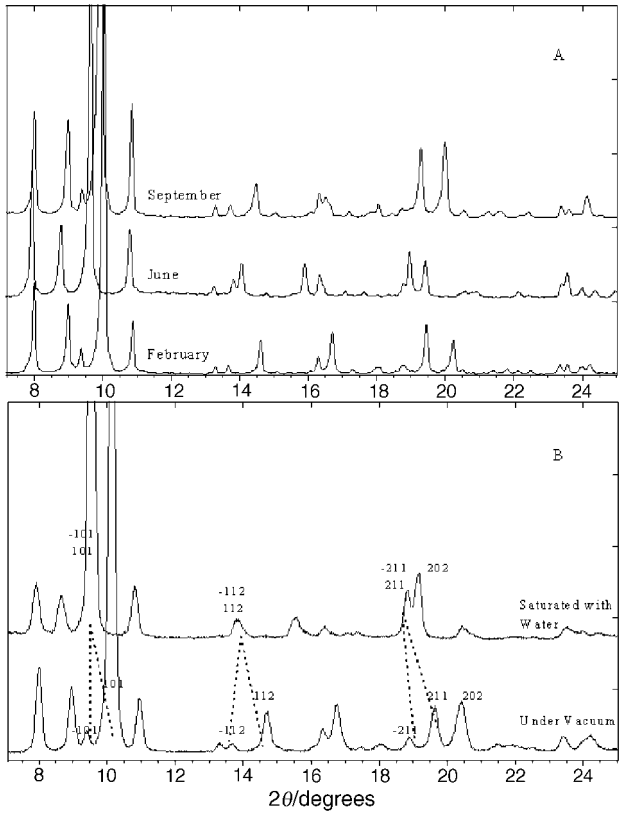

Fig. 4 PXRD patterns of TEA-SnS-1: (A) at different seasons in Toronto, (B) under vacuum and saturated with water

of the ***a*** and ***c*** parameters upon the adsorption of water is actually accompanied by an increase of the interlamellar spacing of up to 0.55 Å. In contrast, the unit cell area of the (202) Miller plane is almost invariant with respect to the adsorption of water, *i.e.* the area of the tin sulfide sheet itself has hardly changed. Therefore, the adsorption of water swells and consequently generates space between the tin(IV) sulfide sheets. This is the well known intercalation phenomenon for a layered structure.[12,13] It can be imagined that the adsorption of larger molecules, like H_2S (3.6 Å) and H_2Se (4 Å), should have resulted in a greater expansion of the interlamellar space. The maximum interlamellar expansion of 0.55 Å upon adsorption of water is however, much smaller than the kinetic diameter of water (2.65 Å).[10] It implies that the adsorbed water molecules are partially residing within the layer plane of the tin sulfide sheets and occupying void space with the 24-atom pores. Note that an intercalation of a 2-D dense packed host material expands the interlamellar spacing typically by the length of the guest molecule. Therefore, the adsorption of water in the TEA-SnS-1 sample is not a pure intercalating process, instead, an integrated process of intercalation and void-filling.

It is evident that the intercalation ability of TEA-SnS-1 allows the inclusion of guest molecules larger than the void spaces existing in the as-synthesized materials. As discovered by the *in situ* FTIR study large H_2S and H_2Se molecules are also included, however the smaller CO guest is discriminated. This indicates that only certain types of guest molecules, like H_2O, H_2S and H_2Se, are able to enter and swell the interlamellar gap of TEA-SnS-1.

The unit cell of ATEA-SnS-1 expands slightly upon adsorption of water, as found in *in situ* PXRD studies shown in Fig. 5. The maximum increase of unit cell volume was found to be 58 $Å^3$ at room temperature, with an interlamellar expansion of 0.09 Å, Table 1. As found in the TEA-SnS-1 structure, the unit cell expansion of ATEA-SnS-1 occurs mainly along the *c* direction, *i.e.* between the tin(IV) sulfide sheets. As shown below, the amount of adsorbed water as determined from the adsorption isotherm under the identical conditions is 3.3% by weight, which is equivalent to 1.4 waters per $(NH_4)_{0.5}(Et_4N)_{1.5}Sn_3S_7$ formula unit or 8.4 water molecules per unit cell. Note that there are six crystallographically equivalent positions in the $P3_121$ space group. The volume of the 8.4 adsorbed water per unit cell can be calculated to be *ca.* 82 $Å^3$, based on the kinetic diameter of water, 1.56 Å. If one assumes that the adsorption of water in the ATEA-SnS-1 sample takes place predominantly on the internal surface of the micropores and the interlamellar surface, and that the contribution from the external surface of crystallites can be neglected, the unit cell voids in ATEA-SnS-1 can be estimated to be 24 $Å^3$, the difference between the total volume (82 $Å^3$) of the adsorbed water molecules and the unit cell volume expansion (58 $Å^3$). The percentage of the free pore volume in ATEA-SnS-1 can be estimated to be 1.4%. Clearly, the adsorption of water in ATEA-SnS-1 is an integrated process of void-filling and intercalating as found for TEA-SnS-1. However, the much smaller interlamellar expansion observed in the ATEA-SnS-1 structure with respect to that of the TEA-SnS-1, implies that

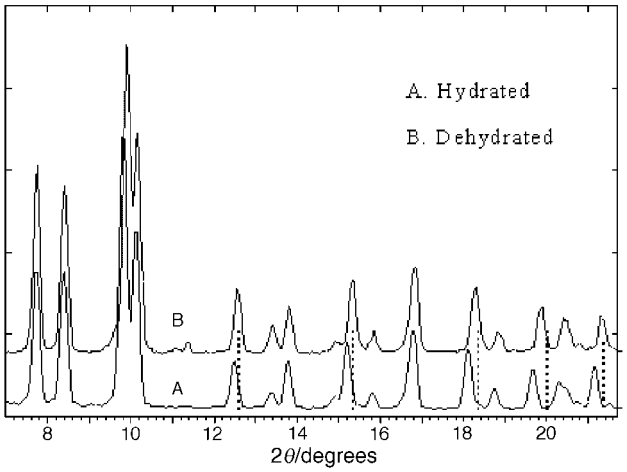

Fig. 5 *In situ* PXRD study of water adsorption by ATEA-SnS-1

Table 1 Unit cell parameters for the two end-members of TEA-SnS-1 and ATEA-SnS-1, calculated from PXRD patterns

	TEA-SnS-1		ATEA-SnS-1	
	dehydrated	hydrated	dehydrated	hydrated
crystal system	monoclinic	pseudo-orthorhombic	trigonal	trigonal
space group	$P2_1/n$	$P2_1/n$	$P3_121$	$P3_121$
a/Å	10.182(2)	10.386(4)	13.246(2)	13.271(3)
b/Å	13.296(3)	13.315(3)		
c/Å	19.779(5)	20.414(8)	26.862(4)	27.138(7)
β/°	95.26(3)	90.11(5)		
V/$Å^3$	2667(1)	2823(2)	4081(1)	4139(1)
interlamellar spacing/Å	8.696(3)	9.250(6)	8.954(2)	9.046(3)

the former has more free void spaces. This is entirely expected based on the single crystal structure of these two materials,[7] which shows that the 24-atom pores in ATEA-SnS-1 $[(NH_4)_{0.5}(Et_4N)_{1.5}Sn_3S_7]$ are less occupied by the Et_4N^+ template cations in comparison with TEA-SnS-1 $[(Et_4N)_2Sn_3S_7]$. A compilation of the unit cell parameter changes of dehydrated TEA-SnS-1 and ATEA-SnS-1 samples upon adsorption of water is shown in Table 1.

In contrast to TEA-SnS-1 and ATEA-SnS-1, the DABCOH-SnS-1 sample does not display any noticeable unit cell changes among as-synthesized, evacuated and water-saturated samples, as demonstrated in Fig. 6, although the *in situ* FTIR and TGA studies have shown that this material reversibly adsorbs water molecules at room temperature. The single crystal XRD structure analysis has also located hydrogen-bonded water molecules inside of the 24-atom pores.[7] This implies that in DABCOH-SnS-1, water molecules are adsorbed entirely within void spaces of the as-synthesized sample, presumably the 24-atom pores of the tin sulfide layer. Therefore, the adsorption–desorption of water molecules does not affect the unit cell parameters. This is consistent with the single crystal structure of DABCOH-SnS-1 in which the $DABCOH^+$ is located between the tin sulfide sheets and the 24-atom pores are empty.[7] Therefore, in contrast to TEA-SnS-1 and ATEA-SnS-1, the adsorption of water in DABCOH-SnS-1 is a pure micropore-filling process. However, this statement does not exclude the possibility of DABCOH-SnS-1 acting as an intercalation host, swelling its constituent layers when exposed to large guests that can interact sufficiently with the framework.

Gas adsorption

H_2O and CO_2 adsorption isotherms of ATEA-SnS-1, obtained on a McBain balance, are displayed in Fig. 7. The as-synthesized ATEA-SnS-1 sample is activated by evacuation at room temperature to remove any physisorbed water molecules. As shown in Fig. 7, the adsorption of water at room temperature follows a type II isotherm.[14] The uptake of water is found to be 3.3 wt.% at 22 Torr water pressure; by stark contrast there is essentially no adsorption of CO_2 at $-78\,^{\circ}C$, Fig. 7.

This confirms that the ATEA-SnS-1 sample selectively adsorbs water and excludes CO_2. It was also found that ATEA-SnS-1 does not adsorb N_2 or Ar at $-196\,^{\circ}C$. The 3.3 wt.% of adsorbed water corresponds to 1.4 water molecules per $(NH_4)_{0.5}(Et_4N)_{1.5}Sn_3S_7$ formula. In contrast to a type I adsorption isotherm which is characteristic for a microporous material, a type II adsorption isotherm is generally indicative of a large external surface area with or without microporosity.[14] For example, a dense material which only has external surface between crystallites, normally exhibits a type II isotherm. So does a blend of dense and microporous materials. When the adsorbent is a layered microporous tin sulfide material, the

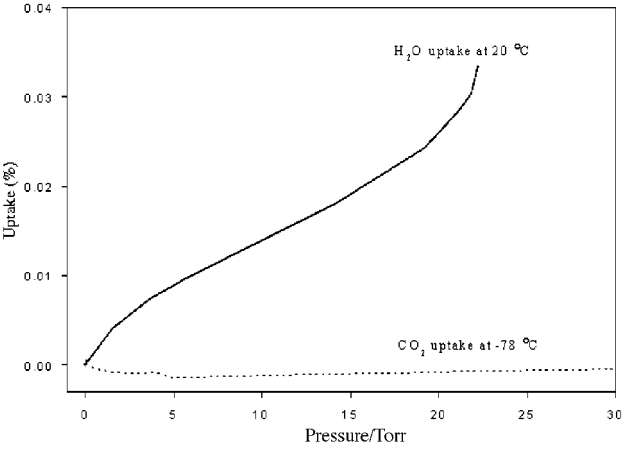

Fig. 7 Adsorption isotherms of ATEA-SnS-1

internal lamellar surface has to be considered in addition to the external surface between crystallites and internal micropore surface. It is actually expected to overwhelm the external surface area if the crystallites contain more than 100 constituent layers like in the SnS-1 materials (*i.e.* with a thickness of more than 0.1 μm). Note that the expansion of interlamellar distance observed by PXRD confirms that the adsorption of water in ATEA-SnS-1 does occur on the internal lamellar surface. Furthermore, intercalation may occur in stages,[14] which in a certain sense is equivalent to a multi-layer adsorption on an external surface. As discussed above, the uptake of water by ATEA-SnS-1 corresponds to combined processes of void-filling and intercalation. This implies that the adsorption of water occurs on the surfaces of the internal micropores and lamellae, therefore expectedly follows a type II adsorption isotherm. It is interesting to note that just like TEA-SnS-1, the ATEA-SnS-1 material also selectively adsorbs water and excludes CO_2, Ar and N_2 although it is capable of swelling its interlamellar space. This again demonstrates that the adsorption properties of the guest molecules play an important role in the molecular recognition process of the SnS-1 materials.

Optical response

The removal of the adsorbed water molecules from the as-synthesized SnS-1 samples induces a red-shift of the optical absorption edge of the SnS-1 materials, as shown in Fig. 8 for an ATEA-SnS-1 sample. Re-exposure of the sample to water causes a reverse blue-shift of the optical absorption edge. The water adsorption–desorption process is reproducible and reversible over many cycles without any noticeable change in the optical spectrum of the material. The magnitude of the

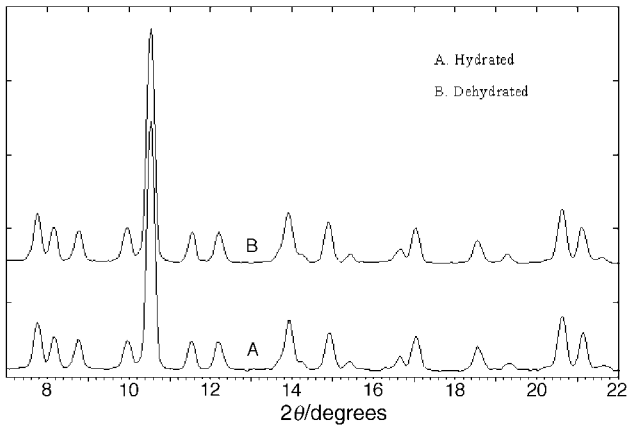

Fig. 6 *In situ* PXRD study of water adsorption by DABCOH-SnS-1

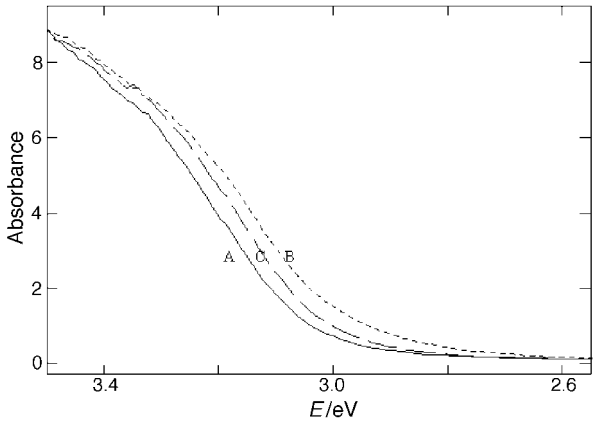

Fig. 8 UV–VIS optical absorption spectra of ATEA-SnS-1: (A) saturated with water, (B) dehydrated and (C) re-exposed to air

optical absorption edge shift corresponds to the amount of adsorbed water. The maximum shift was found to be 0.067 eV for ATEA-SnS-1. Like bulk SnS_2, the optical absorption edge of the SnS-1 material is believed to correspond to an intralayer S^{-II} (3p) to Sn^{IV} (5d) valence to conduction band electronic transition.[15,16] Presumably, the adsorbed water responsible for the red-shift in the absorption edge is hydrogen-bonded to the framework S^{-II}, as established in the single crystal structure of DABCOH-SnS-1.[7] This stabilizes the valence band and widens the band gap, and consequently shifts the optical absorption edge to higher energy.

Electrical response

The electrical response of these materials to the adsorption of guest molecules has been investigated by an *in situ* two-probe dc conductivity measurement. An as-synthesized sample is first evacuated to remove any adsorbed guest molecules, which is indicated by the achievement of a steady resistance value. As depicted in Fig. 9, at room temperature the resistance of an ATEA-SnS-1 sample drops rapidly and dramatically when methanol or water vapor is introduced into the evacuated system. The numerical values are summarized in Table 2. Note the more than 10 million times decrease of sample resistance upon the adsorption of water and methanol molecules. Fig. 10 plots the dependence of an ATEA-SnS-1 sample resistance on the partial pressure (P/P_0) of water vapor in argon. The sample resistance decreases monotonically with an increase of the water vapor pressure. Note that in this case, the evacuated sample chamber was purged with Ar which had been bubbled through distilled water at controlled temperatures below room temperature. A similar sample conductivity increase has been observed at room temperature when NH_3 and EtOH vapors are introduced into the system, the result of which is summarized in Table 2. The guest molecule induced resistance changes were found to be reproducible and reversible over many cycles.

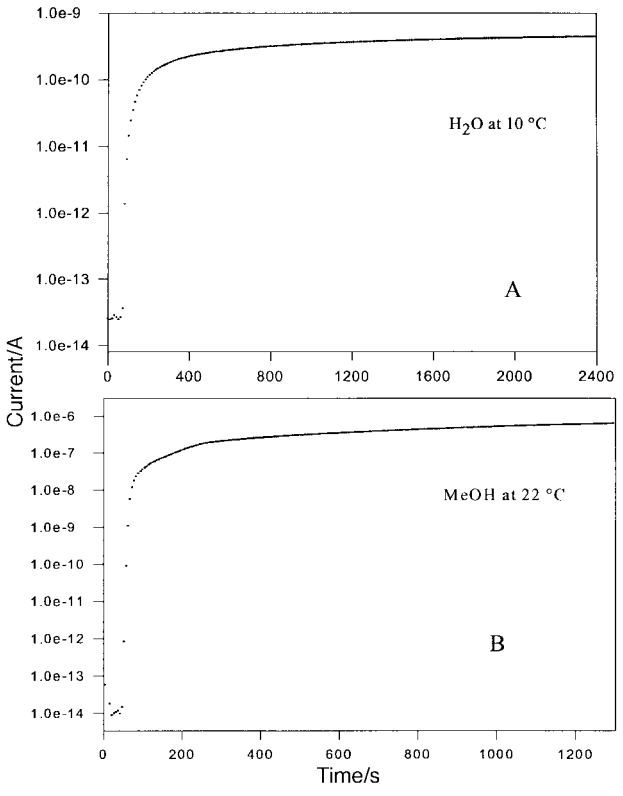

Fig. 9 Illustration of the electrical response of a dehydrated ATEA-SnS-1 sample to the presence of guest molecules. The sample was first activated under vacuum until a constant current was reached, then exposed to (A) water and (B) methanol.

Table 2 A summary of the resistance changes of the TEA-SnS-1 and ATEA-SnS-1 samples induced by guest molecules

guest molecules	pressure/ Torr	ATEA-SnS-1 R_g/R_v[a]	TEA-SnS-1 R_g/R_v[a]	kinetic diameter of guests/Å[10]
NH_3	100	1×10^4	4×10^4	2.6
H_2O	23	6×10^6	2×10^6	2.65
MeOH	108	7×10^7	3×10^8	3.8
EtOH	48	2×10^6	2×10^6	3.8
MeF	80	11	10	N.A.[b]
He	760	10	5	N.A.
H_2	30	10	5	2.89
Ar	760	10	5	3.40
CO_2	760	1	1	3.3

[a] R_g and R_v are the sample resistances in the presence of guest molecules and under vacuum, respectively. [b] N.A.: not available.

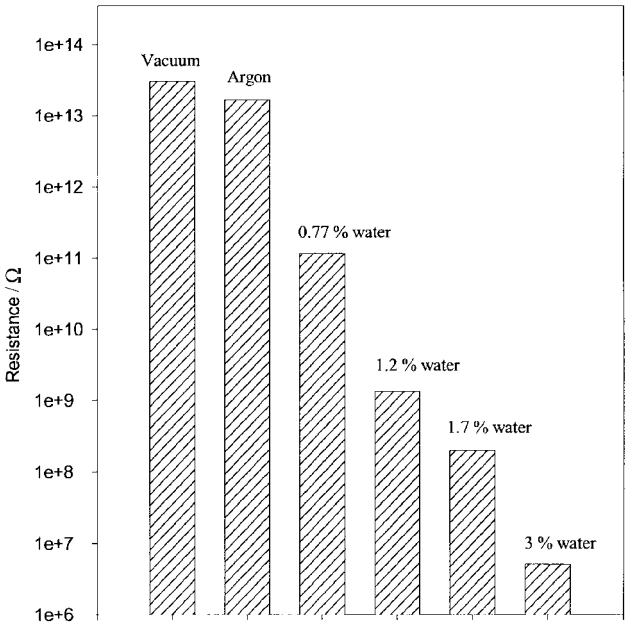

Fig. 10 A representation of the monotonic resistance drop of ATEA-SnS-1 with the increase of the partial pressure of water (P/P_0) in argon

A time response test was designed, in which the sample chamber was flipped open between a mixture of (0.77% H_2O in Ar) and (3.0% H_2O in Ar) in every 30 s through a three-way valve, as demonstrated in Fig. 11. It is evident that the response of an ATEA-SnS-1 sample to the change of water partial pressure is fast, within several seconds.

Interestingly, the conductivity of both TEA-SnS-1 and ATEA-SnS-1 samples remains essentially invariant in CO_2, H_2, Ar, He, and even in MeF which has a large dipole moment of 1.851 D,[17] see Table 2. Clearly, the SnS-1 materials are able to selectively detect the presence and concentration of certain types of guest molecules. The selectivity does not seem to be related to the size or shape differences of the guest molecules, but rather to their adsorption properties. For example, although both CO_2 and MeF are excluded, they are considerably smaller than EtOH which is recognized by both SnS-1 samples. A comparison of the kinetic diameters[10] of the guest molecules is listed in Table 2. The nature of the guest molecules and their specific interaction with the tin(IV) sulfide framework appear to plays a key role in the adsorption–transducer action.

Discussion

Combining all of the results described above obtained from the *in situ* FTIR and PXRD studies, gas adsorption isotherms, optical and electrical measurements, one concludes that the

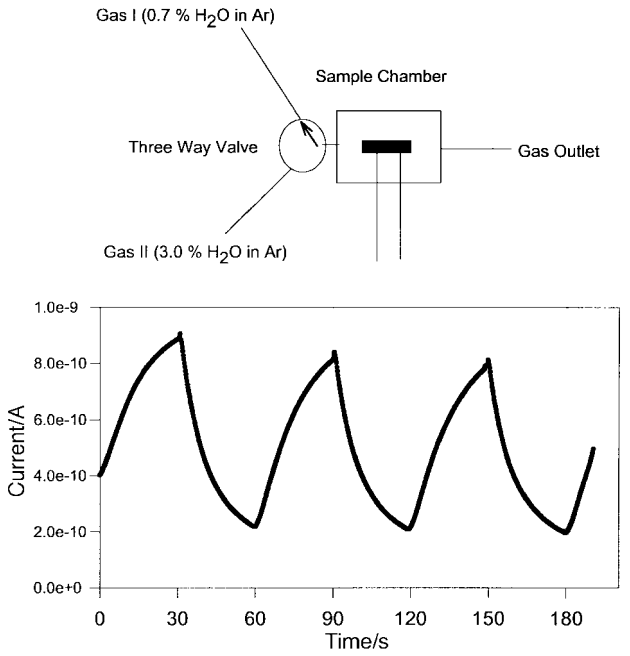

Fig. 11 A plot of the electrical response *vs.* time of ATEA-SnS-1 to the change of water partial pressure in argon

adsorption behavior of SnS-1 materials is rather complicated. It appears that molecules such as H_2, He, N_2, Ar, CO and CO_2, can only be adsorbed as void-fillers and have to be smaller than the free micropore space existing in the layers of the original SnS-1 structure. On the other hand, molecules like H_2O and H_2S can be adsorbed through a combination of micropore-filling and intercalation. Also the adsorption is not limited by molecular size and shape. As an example, ATEA-SnS-1 excludes CO_2 molecules but includes H_2O following a type II isotherm; while the uptake of both CO_2 and H_2O in TMA-SnS-1 has been reported to follow a type I adsorption isotherm and to be a pure micropore-filling process.[18] The TMA^+ template cations in TMA-SnS-1 are found to reside in the gap between the tin sulfide sheets and the 24-atom pores within the tin sulfide sheets are empty.[19] In contrast, the TEA^+ cations in ATEA-SnS-1 are extended into the 24-atom pores.[7] Therefore, compared to ATEA-SnS-1, the TMA-SnS-1 structure should contain more free void volume that is able to accommodate CO_2 and H_2O molecules without needing to swell the tin sulfide sheets to generate extra space. However, the free void volume in ATEA-SnS-1 is small relative to the size of CO_2 and H_2O, and due to the different adsorption behavior of these two molecules, the former is excluded and the latter is adsorbed with the assistance of intercalation. Note that TMA-SnS-1 has also been reported to discriminate Ar, the kinetic diameter of which is 3.40 Å, only 0.1 Å larger than CO_2.[18] This clearly shows that the SnS-1 materials can function as a molecular sieve towards certain molecules. In the case of TEA-SnS-1, which has even less free void space compared with ATEA-SnS-1, the uptake of water molecule causes a greater swelling of the interlamellar gap by as much as 0.55 Å. This indicates that through intercalation, the incorporation of large molecules in these layered microporous materials is entirely possible. This is to be contrasted with 3-D open-framework zeolites that discriminate molecules based on the geometric dimensions and specific adsorption in the pores.[10] TEA-SnS-1 is also found to be able to adsorb H_2S and H_2Se molecules, presumably causing a greater interlamellar expansion than 0.55 Å. Clearly, the adsorption of guest molecules in the microporous layered tin sulfide materials is controlled not only by guest molecule size relative to the free void volume present in the structure but also by their adsorption properties.

It seems that molecules which have a hydrogen-bonding ability, such as NH_3, H_2O, H_2S, H_2Se, MeOH and EtOH are particularly favored for adsorption by the SnS-1 materials. Presumably, these molecules can interact strongly with SnS-1 by hydrogen bonding to the framework sulfur, which might be the driving force for intercalation reactions. For non-polar molecules that cannot form hydrogen bonds with the framework, the adsorption is controlled more by molecule size/shape, and the SnS-1 materials behave as molecular sieves towards them. Interestingly, MeF, a molecule with a large dipole moment of 1.85 D but low polarizability, induced barely any resistance change to the SnS-1 materials, suggesting that it is also excluded.

The observed 10 million-fold change of conductivity of the TEA-SnS-1 and ATEA-SnS-1 samples in the presence of guest molecules like H_2O, MeOH and EtOH, is of great interest for sensing applications. The magnitude of the guest-induced resistance change of the SnS-1 materials is comparable to that found in commercial semiconductor sensors. For example, the sensitivity of a SnO_2-based H_2S sensor is about 10^2–10^3 in the presence of 5 ppm H_2S, and a SnO_2-based NO_2 sensor is about 10–10^2 in the presence of 200 ppm NO_2.[20–22] At this time however, the mechanism responsible for the guest-induced conductivity changes of the SnS-1 material is not clear. Electrical conduction occurs by a long range movement of either electrons or ions.[23,24] In most situations, one type of charge carrier is predominant, however, in some materials, both electronic and ionic conduction can be important. The conductivity formula is $\sigma = \Sigma n_i e_i \mu_i$, where n_i is the number of charge carriers of species i, e_i is the charge of i, and μ_i the mobility of i. Therefore conductivity increases with the number of charge carriers and their mobility. In the SnS-1 materials, the ionic conductivity seems to be insignificant as the movement of template cations, like NH_4^+ and Et_4N^+, is expected to be sluggish. This proposal is supported by the observation that all of the SnS-*n* materials with distinct template size and void volume, like DABCOH-SnS-1, ATEA-SnS-1, TEA-SnS-1 and TPA-SnS-3, display very similar conductivity changes under identical experimental conditions. In the case of ionic conductivity, smaller cations generally give rise to greater conductivity as they are more mobile than larger cations, although in certain circumstances, smaller cations may have a high ionic potential causing them to interact more strongly with the framework and therefore move more slowly than larger cations. Considering the observation that the guest molecules which have induced a conductivity change of the SnS-1 materials are all able to hydrogen-bond with the tin sulfide framework, one might believe that a protonic conductivity is involved. However, the measured sample conductivity change was invariant when the gaseous mixture of H_2O–Ar was replaced by H_2–H_2O–Ar, having the same vapor pressure of water. Note that in these measurements more reactive porous Pt electrodes were employed. The samples were pressed into a thin pellet with a thickness of *ca.* 1–2 mm, sputtered with a thin layer of Pt metal on both sides, and then held together tightly by two pieces of Pt mesh. Protons are known to be generated from adsorption-induced dissociative-ionization of hydrogen gas on the surface of the porous Pt anode when a small voltage of a couple of volts is applied. In the case of a proton-conductor, a rise of conductivity is expected owing to the increase of H^+, *i.e.* the charge carrier concentration. The result of no observable difference between H_2O–Ar and H_2–H_2O–Ar mixtures suggests that protonic transport in the SnS-1 materials is not a significant contributor to the measured conductivity. To test the possibility of NH_4^+ conductivity in ATEA-SnS-1, sample conductivity changes were measured using NH_3–Ar and NH_3–H_2–Ar mixtures as guest molecules under identical experimental conditions. However, a very similar conductivity change was observed again even though NH_4^+ cations are known to be formed at the porous

Pt anode in the presence of NH_3–H_2–Ar through the reaction of NH_3 and H^+, and an increased conductivity is expected if NH_4^+ ion conductivity is involved.

These experimental results do not support an ionic conductivity mechanism. The other possibility is an electronic conductivity mechanism. If electronic transport is really occurring, the observed increase of conductivity implies that the band structure of the SnS-*n* materials has somehow been modified by the adsorbed guest molecules to create charge carriers. One possibility is that due to hydrogen bonding between the adsorbed molecules and the SnS-*n* framework, an empty antibonding orbital from the acceptor guest molecule is formed at an energy level higher than the valence band of the SnS-1 material, *i.e.* the donor band, by about 1.5 kcal mol^{-1}, the approximate energy of a $S-H_2O$ hydrogen bond.[11] At room temperature, such acceptor states might be significantly populated, leaving an equivalent number of holes in the sulfur valence band. In a certain sense, this is related to the p-doping process of semiconductors which increases the density of hole carriers in the valence band and consequently the conductivity of the sample. From this point of view, the charge-transfer conductivity mechanism proposed here for the SnS-*n* materials is similar to that operating in many metal-oxide semiconductor sensory materials, like SnO_2, which is believed to detect gaseous molecules *via* adsorption-induced charge-transfer processes that alters the density of carriers and thus the conductivity of the sample.[20–22] It should be mentioned however, that there is an important distinction between the bulk semiconductor SnO_2 and the microporous layered SnS-*n* materials, since a dominant space charge region can exist in the latter. The electrical resistance of the SnS-*n* materials could be more sensitive to adsorbed guests as the Debye (charge depletion) length may be comparable to the tin(IV) sulfide microporous layer thickness. It is clear that more studies are required to elucidate details of the mechanism of adsorbate-induced charge-transport in SnS-*n* materials.

Conclusion

Microporous layered SnS-1 materials are found to selectively and reversibly adsorb certain molecules. A pure micropore-filling process is observed for the uptake of small non-polar guest molecules, however, for certain large guests an integration of micropore-filling and intercalation occurs. The former is controlled by the size of guest molecules, while the latter depends on the adsorption properties of guest molecules. It seems that guest molecules which have a propensity for hydrogen bonding are favored for intercalation. The SnS-1 structures are found to flex reversibly upon the adsorption–desorption of guest molecules, due to cooperative reconstruction of the microporous layers and the positions of template cations. The fast and large electrical response of these materials to adsorbed guests make them attractive candidates for chemoselective sensing applications. The observed sensitivity, reversibility and fast reaction times are comparable to some commercial semiconductor sensors. The sensitivity of the SnS-1 materials to NH_3, H_2S and alcohols makes them interesting for environmental, industrial and biomedical monitoring applications. An 'electronic nose' may be built from an array of molecule discriminating R-SnS-*n* materials, containing different charge-balancing cations distributed in particular ways in the micropore and interlayer spaces. Unique response patterns obtained for different gas mixtures should further enhance the selectivity and sensitivity of this class of materials for sensing applications.[25]

Experimental

Reagents

Synthetic, structural, thermochemical and spectroscopic properties of TEA-SnS-1, ATEA-SnS-1 and DABCOH-SnS-1 have recently been described.[5–9,27] For guest-induced sample conductivity measurements, anhydrous NH_3, high purity Ar, extra dry N_2, CO_2, CO and pre-analyzed 1% H_2 in He were purchased from Canox, and Semiconductor 2.5 purity MeF from Matheson. Anhydrous MeOH and EtOH were prepared by refluxing MeOH in magnesium methoxide and EtOH in magnesium ethoxide for 3 days and then distilled and stored under extra dry Ar.

Physical measurements

Diffuse reflectance UV–VIS spectra were collected using a Cary 3 double beam spectrophotometer with powder samples packed in an *in situ* quartz cell and referenced to an Oriel Corporation 1-SRS-99–010 Spectralon White Standard. The de-hydrated sample was prepared by evacuation to remove any physisorbed molecules. The spectra were converted to absorbance units using the Kubelka–Munk transformation of the reflectance data. *In situ* PXRD patterns were recorded on a Siemens D-5000 diffractometer. The samples were activated by evacuation at elevated temperatures below the decomposition temperature.[5–9,27] Water-saturated samples were obtained by bubbling nitrogen through distilled water before entering the sample chamber. FT-mid-IR spectra were recorded on self-supporting wafers mounted within an *in situ* cell using a Nicolet 20SXB spectrometer. Adsorption isotherms were collected using a McBain balance with H_2O at 25 °C, CO_2 at −78 °C, Ar and N_2 at −196 °C. A 99.8% pure Al_2O_3 tube (Vesuvius McDanel, 998A-3100, 0.25 in od) was used as a substrate for electrical measurements. Two shallow grooves, 1 mm apart, were cut into the tubes. Gold or platinum wires (25/1000 in diam.) were wrapped tightly around the alumina tubes. A slurry of the powder sample was applied around the substrate tube. The thickness of the sample was estimated to be *ca.* 1 mm. Resistance measurements were carried out employing a HP 4140 picoammeter/DC voltage source. Special precaution was taken to minimize any current leakage and/or interference from any outside source. Typically 10–20 V of potential difference was applied across the sample and the resulting current was measured. For adsorption-induced conductivity experiments, the sample chamber was first evacuated until a steady resistance value was obtained, then switched open to a gaseous or liquid adsorbate source. Alternatively, a flow of Ar was bubbled through a liquid adsorbate and then to the sample chamber. The flow of the gas through the liquid absorbate was maintained sufficiently slow to ensure saturation. The temperature of the liquid adsorbate was controlled using a Neslab RTE-111 microprocessor controller refrigerated bath/circulator. The partial pressure of water, MeOH and EtOH vapor was calculated using thermodynamic data by Gaskell.[26]

G.A.O. is deeply indebted to the Killam Foundation for an Issac Walton Killam Research Fellowship, 1995–97. The Natural Sciences and Engineering Research Council of Canada (NSERC), Universal Oil Products (UOP) and the Canadian Space Agency (CSA) are also acknowledged for their generous financial support of this work. T.J. is grateful for graduate scholarships from the University of Toronto. The assistance of Mr Greg Vovk with the McBain balance adsorption isotherm measurements is deeply appreciated. Dr Srebri Petrov is also acknowledged for his expert help with the analysis of the PXRD patterns.

References

1 J. M. Newsam, *Science*, 1986, **231**, 1093; J. M. Thomas, *Angew. Chem. Int. Ed. Engl.*, 1988, **27**, 1673.
2 G. A. Ozin, *Adv. Mater.*, 1992, **4**, 612; T. E. Mallouk and D. J. Harrison, in *Interfacial Design and Chemical Sensing*, ACS

Symposium Series 561, American Chemical Society, Washington, DC. 1994.
3 T. Bein, *Chem. Mater*., 1996, **8**, 1636; K. Brown, T. Bein, G. C. Frye and C. J. Brinker, *J. Am. Chem. Soc*., 1989, **111**, 7640; Y. Yan and T. Bein, *Mater. Res. Soc. Symp. Proc*., 1991, **233**, 175; Y. Yan and T. Bein, *J. Phys. Chem*., 1992, **96**, 9387; Y. Yan and T. Bein, *Chem. Mater*., 1992, **4**, 975.
4 K. J. Balkus, L. J. Ball, B. E. Gnade and J. M. Anthony, *Chem. Mater*., 1997, **9**, 380.
5 H. Ahari, R. L. Bedard, C. L. Bowes, T. Jiang, G. A. Ozin and D. Young, *US Pat*., 5594263, 1997.
6 T. Jiang, A. Lough and G. A. Ozin, *Adv. Mater*., 1998, **10**, 42.
7 T. Jiang, R. L. Bedard, R. Broach, A. Lough and G. A. Ozin, *J. Mater. Chem*., 1998, **8**, 721.
8 T. Jiang, G. A. Ozin, R. L. Bedard and A. Lough, *J. Mater. Chem*., 1998, **8**, 733.
9 C. L. Bowes, S. Petrov, G. Vovk, D. Young, G. A. Ozin and R. L. Bedard, *J. Mater. Chem*., 1998, **8**, 711.
10 D. W. Breck, *Zeolite Molecular Sieves: Structure, Chemistry, and Use*, John Wiley & Sons, New York, 1974.
11 D. F. Shriver, P. Atkins and C. H. Langford, *Inorganic Chemistry*, W. H. Freeman, New York, 1994.
12 *Intercalation Chemistry*, ed. M. S. Whittingham and A. J. Jacobson, Academic Press, New York, 1982.
13 D. O'Hare, in *Inorganic Materials*, ed. D. O'Hare and D. W. Bruce, John Wiley & Sons, Chichester, 1992, ch. 4.
14 S. Gregg and K. S. W. Sing, *Adsorption, Surface Area and Porosity*, Academic Press Inc., New York, 2nd edn., 1982
15 J. Robertson, *J. Phys. C: Solid State Phys*., 1979, **12**, 4735.
16 E. Lifshitz, Z. Chen and L. Bykov, *J. Phys. Chem*., 1993, **97**, 238.
17 W. Braker and A. L. Mossman, *Matheson Gas Data Book*, Matheson Division Searle Medical Products USA Inc, Lyndhurst, NJ 07071, 6th edn., 1980, p. 476.
18 R. L. Bedard, L. D. Vail, S. T. Wilson and E. M. Flanigen, *US Pat*., 4880761, 1989; 4933068, 1990; C. B. Bowes, Ph.D. Thesis, University of Toronto, 1996.
19 J. B. Parise, Y. Ko, J. Rijssenbeek, D. M. Nellis, K. Tan and S. Koch, *J. Chem. Soc., Chem. Commun*., 1994, 527.
20 M. Ando, S. Suto, T. Suzuki, T. Tsuchida, C. Nakayama, N. Miura and N. Yamazoe, *J. Mater. Chem*., 1994, **4**, 631.
21 G. S. V. Coles, *8th International School on Condensed Matter Physics, Sept., 1994*, Bulgaria, *Chem. Eng. News*., 1994, Oct. 3, 40.
22 H. M. Azad, S. A. Akbar, S. G. Mlaisaker, L. D. Birefeld and K. S. Goto, *J. Electrochem. Soc*., 1992, 3690.
23 A. Hamnett, in *Solid State Chemistry Techniques*, ed. A. K. Cheetham and P. Day, Oxford University Press, New York, 1987, ch. 8.
24 A. R. West, *Solid State Chemistry and Its Applications*, John Wiley & Sons Ltd., 1989, ch. 15.
25 L. Moy and M. Collins, *Am. Lab*., Feb. 1996, 22; T. A. Dickinson, J. White, J. S. Kauer and D. R. Walt, *Nature* (*London*), 1996, **382**, 697; M. C. Lonergan, E. J. Severin, B. J. Doleman, S. A. Beaber, R. H. Grubbs and N. S. Lewis, *Chem. Mater*., 1996, 8, 2298.
26 D. Gaskell, *Introduction to Metallurgical Thermodynamics*, Washington Hemisphere Pub. Corp., New York, 2nd edn., 1981.
27 T. Jiang, G. A. Ozin and R. L. Bedard, *J. Mater. Chem*., preceding paper.

Paper 8/01501E; *Received* 23*rd February*, 1998